

PAPER

Extended Beamforming by Sum and Difference Composite Co-Array for Real-Valued Signals

Sho IWAZAKI[†], *Student Member* and Koichi ICHIGE^{†a)}, *Member*

SUMMARY We have developed a novel array configuration based on the combination of sum and difference co-arrays. There have been many studies on array antenna configurations that enhance the degree of freedom (DOF) of an array, but the maximum DOF of the difference co-array configuration is often limited. With our proposed array configuration, called “sum and difference composite co-array”, we aim to further enhance the DOF by combining the concept of sum co-array and difference co-array. The performance of the proposed array configuration is evaluated through computer simulated beamforming*.

key words: adaptive beamforming, extended array signal processing, correlation matrix

1. Introduction

Adaptive beamforming by array antenna plays an important role in radar, sonar, indoor, and outdoor wireless communications [1]–[3]. Direction-of-arrival (DOA) estimation is also an effective technique to accurately detect the directions of array input signals, and several accurate algorithms for doing so have been proposed [4]–[6]. These methods are based on the eigenvalue decomposition of the sample covariance matrix of the array input signal, which can be regarded as algorithms with the degree of freedom (DOF) of $O(N)$, where N denotes the number of antenna elements.

There have been many studies on minimum redundancy arrays (MRAs) and methods using fourth-order cumulants in order to enhance the DOF [7]. However, MRAs often require very complicated computation for optimizing the array configuration. Also, the fourth-order cumulant approach can be utilized only for non-Gaussian signals. The concept of the Khatri-Rao (KR) product [8] assumes a quasi-stationary process and gives a difference co-array (which forms part of a larger virtual array aperture) with the DOF of $(2N - 1)$, but it cannot be used with the stationary process. Nested and co-prime arrays [9]–[12] have attracted attention as a version of the difference co-array, and the two-level nested array can achieve the DOF of $O(N^2)$. However, the maximum DOF of these configurations based on the difference co-array is limited to $N(N - 1) + 1$.

In this paper, we present a novel array configuration called “sum and difference composite co-array” that combines the sum and difference co-arrays to further extend the

DOF of the difference co-array. We introduce the sum co-array on the receiver side and combine the sum and difference co-arrays to enable this configuration. Using the sum and difference co-arrays together in a co-prime array has been proposed before [13]–[16], but our approach enables an array configuration with a longer continuous part in a virtual array, thus resulting in a higher DOF than the co-prime configuration [17], [18]. In addition, we can make the sum co-array part with lower calculation cost because no temporal autocorrelations of the array inputs are required. Our aim is to develop a physical and virtual array configuration that exceeds the maximum DOF of the difference co-array. Moreover, most of the conventional sum and difference co-arrays evaluate DOA estimation and/or beamforming performance without transmission/reception system configuration. We have developed digital modulation/demodulation scheme for the proposed co-array, its transmission/reception system configuration, and evaluated digital communication performance by means of bit error ratio (BER).

The rest of the paper is organized as follows. In Sect. 2 of this paper, we briefly introduce the signal models of a general array antenna and the difference co-array configurations. Section 3 describes the concept of the proposed sum and difference composite co-array, and then Sect. 4 discusses its application to beamforming. After presenting the simulation results in Sect. 5, we conclude with a brief summary and mention of future work in Sect. 6.

2. Preliminaries

In this section, we first prepare the basic signal model of the difference co-array. Then we introduce a matrix rank restoration technique based on spatial smoothing.

2.1 Signal Model of Difference Co-Array

Consider an N elements uniform linear array (ULA) with the signal model given by $N \times 1$ array steering vector $\mathbf{a}(\theta)$ corresponding to the phase delays of each array input $e^{j(2\pi/\lambda)d_p \sin \theta}$ that come from the direction of θ ; at the p -th element. Here, the parameter λ is the wavelength of the carrier wave and $d_p = p \cdot d$ is the distance between the reference (first) and the p -th element positions where $d = \lambda/2$.

We assume D narrowband input waves impinging on

Manuscript received December 11, 2018.

Manuscript revised March 8, 2019.

[†]The authors are with Department of Electrical and Computer Engineering, Yokohama National University, Yokohama-shi, 240-8501 Japan.

a) E-mail: koichi@ynu.ac.jp

DOI: 10.1587/transfun.E102.A.918

*Preliminary versions of this manuscript have been presented in [17], [18].

this array with the powers $\{\sigma_i^2, i = 1, 2, \dots, D\}$ from the directions $\{\theta_i, i = 1, 2, \dots, D\}$, respectively; then, the received signal vector $\mathbf{x}(k) = [x_1(k), x_2(k), \dots, x_N(k)]^T$ is written as

$$\mathbf{x}(k) = \mathbf{A}s(k) + \mathbf{n}(k), \quad (1)$$

where the matrix $\mathbf{A} = [\mathbf{a}(\theta_1), \mathbf{a}(\theta_2), \dots, \mathbf{a}(\theta_D)]$ expresses the array manifold matrix and $s(k) = [s_1(k), s_2(k), \dots, s_D(k)]^T$ is the plane source signal vector of which signals $s_i(k)$ are uncorrelated to each other and temporally uncorrelated with itself. Its elements generally take complex values. The vector $\mathbf{n}(k) = [n_1(k), n_2(k), \dots, n_N(k)]^T$ is a noise vector that has temporally and spatially white Gaussian signals that are uncorrelated to each other in this case. The autocorrelation matrix of the array input vector $\mathbf{x}(k)$ is denoted as

$$\begin{aligned} \mathbf{R}_{xx} &= E[\mathbf{x}(k)\mathbf{x}^H(k)] \\ &= \mathbf{A}\mathbf{R}_{ss}\mathbf{A}^H + \sigma^2\mathbf{I}_N \\ &\simeq \mathbf{A} \begin{bmatrix} \sigma_1^2 & & & O \\ & \sigma_2^2 & & \\ & & \ddots & \\ O & & & \sigma_D^2 \end{bmatrix} \mathbf{A}^H + \sigma^2\mathbf{I}_N, \end{aligned} \quad (2)$$

where $\mathbf{R}_{ss} = E[s(k)s^H(k)] \in \mathbb{R}^{D \times D}$, $\mathbf{A} \in \mathbb{C}^{N \times D}$, σ^2 denotes the noise power and $\mathbf{I}_N \in \mathbb{R}^{N \times N}$ denotes the identity matrix. Then, we vectorize the matrix \mathbf{R}_{xx} as

$$\begin{aligned} \mathbf{z} &= \text{vec}(\mathbf{R}_{xx}) \\ &= \text{vec} \left\{ \sum_{i=1}^D \sigma_i^2 (\mathbf{a}(\theta_i)\mathbf{a}^H(\theta_i)) \right\} + \sigma^2\mathbf{1}_N \\ &= (\mathbf{A}^* \odot \mathbf{A})\mathbf{p} + \sigma^2\mathbf{1}_N, \end{aligned} \quad (3)$$

where $\mathbf{1}_N = [\mathbf{e}_1^T, \mathbf{e}_2^T, \dots, \mathbf{e}_N^T]^T \in \mathbb{R}^{N^2 \times 1}$, $\mathbf{p} = [\sigma_1^2, \sigma_2^2, \dots, \sigma_D^2]^T \in \mathbb{R}^{D \times 1}$, and \odot denote the Khatri-Rao product operator. The unit vector $\mathbf{e}_i \in \mathbb{R}^{N^2 \times 1}$ consists of the following components: i -th column being one, and all the others being zero.

It is important that the column component of $\mathbf{A}^* \odot \mathbf{A} \in \mathbb{C}^{N^2 \times D}$ enable us to represent the extended array steering vector, which includes the set of virtual sensor positions $\{d_p - d_q \mid 1 \leq p, q \leq N\}$. This form is called the difference co-array and can be applied to DOA estimation, adaptive beamforming, and so on. Also, the difference co-array behaves in accordance with the second-order statistics of the input vector, such that σ_i^2, σ_j^2 ($i \neq j$) behave like coherent signals to each other. An earlier study [9] showed that the maximum DOF in that case is given by $\text{DOF}_{\text{Diff-Max}} = N(N-1) + 1$.

Furthermore, we remove redundant rows from the above manifold $\mathbf{A}^* \odot \mathbf{A}$, replace the rows that correspond to the locations of virtual elements in ascending order. Let denote this matrix as $\mathbf{A}_1 \in \mathbb{C}^{N_1 \times D}$, where $N_1 = N^2/2 + N - 1$ in case of even N [9]. Then, the new observation vector $\mathbf{z}_1 \in \mathbb{C}^{N_1 \times 1}$ whose elements are in order without redundancy is given by

$$\mathbf{z}_1 = \mathbf{A}_1\mathbf{p} + \sigma^2\hat{\mathbf{e}}, \quad (4)$$

where $\hat{\mathbf{e}} \in \mathbb{R}^{N_1 \times 1}$ is a vector of all zeros except a 1 at the $(N^2/4 + N/2)$ -th position [9].

2.2 Rank Restoration by Diagonal Loading

The correlation matrix may become singular and then there will be some problems of stability or accuracy. Therefore we often add a constant to the diagonal elements of the target matrix \mathbf{R}_{xx} so that the matrix become non-singular. This rank restoration approach is called as Diagonal Loading (DL) and formulated as

$$\mathbf{R}_{\text{DL}} = \mathbf{R}_{xx} + \delta\mathbf{I}_N, \quad (5)$$

where δ is an adjustment factor. The DL approach does not require a spatially smoothed matrix. This will lead to a more robust beamforming performance, as seen in the next section, and also has the great advantage that we can keep the DOF without any spatial smoothing method.

3. Proposed Approach

In this section, we present our novel array configuration, the ‘‘sum and difference composite co-array’’, and show its numerical model. The concept of the sum co-array assumes that we can manage both the transmitter and receiver sides, similar to the well-known MIMO system, and then a set of virtual arrays (channels) $\{\mathbf{x}_{Tp} + \mathbf{x}_{Rq} \mid 1 \leq p \leq M, 1 \leq q \leq N\}$ can be realized, where M and N denote the number of transmitters and receivers, respectively. Under the above condition, $(M + N)$ array elements enable the DOF of MN .

The sum co-array can also be realized by the receiver side only, via algebraic operation, as discussed later. Our aim with the proposed sum and difference composite co-array is to achieve a higher DOF than that of the difference co-array, $\text{DOF}_{\text{Diff-Max}} = N(N-1) + 1$.

3.1 Definition of Correlation Matrix

As discussed in Sect. 2, the core procedure when generating the difference co-array is to deduce the vectorized autocorrelation matrix $\text{vec}(\mathbf{R}_{xx})$. For simplification, we modify the expression of \mathbf{z} in (3) as

$$\begin{aligned} \mathbf{z} &= \text{vec}(\mathbf{R}_{xx}) \\ &= \text{vec} \left\{ \sum_{i=1}^D \sigma_i^2 (\mathbf{a}(\theta_i)\mathbf{a}^H(\theta_i)) \right\} + \sigma^2\mathbf{1}_N \\ &= \left\{ \sum_{i=1}^D \sigma_i^2 (\mathbf{a}^*(\theta_i) \otimes \mathbf{a}(\theta_i)) \right\} + \sigma^2\mathbf{1}_N. \end{aligned} \quad (6)$$

The key fact here is that the manifold $(\mathbf{a}^*(\theta_i) \otimes \mathbf{a}(\theta_i))$ represents the array steering vector of the virtual elements that compose the difference co-array.

For example, consider a 6-element nested array with the physical sensor location $\{0, 1, 2, 3, 7, 11\}$, which is a kind of difference co-array. We see that the relation



Fig. 1 Construction of 6-element nested array.

$$a_p^*(\theta_i)a_q(\theta_i) = a_{q-p}(\theta_i) \quad (7)$$

holds, where $p, q = \{0, 1, 2, 3, 7, 11\}$. In the case of $p = 2$ and $q = 7$, a complex virtual array component $a_2^*(\theta_i)a_7(\theta_i) = a_5(\theta_i)$ can be obtained at the location $q - p = 7 - 2 = 5$. The configuration of the 6-element nested array is shown in Fig. 1, where the black and gray elements respectively mean real (physical) and virtual array elements.

Now, we adopt the concept of the sum co-array. Its original concept is to generate a virtual array element at $(p + q)$ -th location for any physical location p and q . We start from the relation

$$a_{q+p}(\theta_i) = a_p(\theta_i)a_q(\theta_i), \quad (8)$$

and trace back the deduction process of the extended array, i.e.,

$$\begin{aligned} & \left\{ \sum_{i=1}^D \tilde{\sigma}_i^2 (\mathbf{a}(\theta_i) \otimes \mathbf{a}(\theta_i)) \right\} + \tilde{\sigma}^2 \mathbf{1}_N \\ &= \text{vec} \left\{ \sum_{i=1}^D \tilde{\sigma}_i^2 (\mathbf{a}(\theta_i) \mathbf{a}^T(\theta_i)) \right\} + \tilde{\sigma}^2 \mathbf{1}_N \\ &= \text{vec}(\tilde{\mathbf{R}}_{xx}) =: \tilde{\mathbf{z}}, \end{aligned} \quad (9)$$

where $\tilde{\sigma}_i^2$ and $\tilde{\sigma}^2$ respectively denote the i -th impinging signal power and the noise power. Assume that the desired wave takes real values that satisfy $s_s(k) = s_s^*(k)$, as in [13]. That is, the relation $\tilde{\sigma}_1^2 = \sigma_1^2$ holds and we can realize the sum co-array for the desired signal. In this case, the matrix $\tilde{\mathbf{R}}_{xx}$ is written as

$$\tilde{\mathbf{R}}_{xx} = E[\mathbf{x}(k)\mathbf{x}^T(k)] = \mathbf{A}\tilde{\mathbf{R}}_{ss}\mathbf{A}^T + \tilde{\sigma}^2\mathbf{I}_N, \quad (10)$$

where $\tilde{\mathbf{R}}_{ss}$ is the correlation matrix corresponding to the real-valued signal $\tilde{\mathbf{s}}$. Then, the observation vector $\tilde{\mathbf{z}}$ in (9) is regarded as the extended array steering vector of the sum co-array.

3.2 Sum and Difference Composite Co-Array

We investigate how the DOF can be enhanced to more than that of the difference co-array by combining the sum co-array model described in Sect. 3.1 with the difference co-array. As stated above, the observation vector $\tilde{\mathbf{z}}$ of the sum co-array can be derived by a similar process to the difference co-array, provided that the signal $s_s(k)$ takes a real value.

Now, we examine the formulation of array configuration $\{d_p \mid 0 \leq p \leq N - 1\}$. The key concept is to use not only the difference components but also the sum components and not to generate any hole (position lacking any physical element). For the nested array, we first divide the array into multiple groups. In the case of a 2-level array configuration where N is even, the array sensors can be divided into

2 groups, both of which have $N/2$ elements. Assume that 1st-group is allocated from d_0 to $d_{N/2-1}$ at intervals of d : expressed as $\{d_p = pd \mid 0 \leq p \leq N/2 - 1\}$, the virtual components including the sum ones are generated up to d_{N-2} continuously. We also consider the allocation of 2nd-group $\{d_{\alpha_p} \mid 1 \leq p \leq N/2\}$, where α_p is given as $\{N/2 + p(N - 1)\}$, d_{α_p} means p -th position in 2nd-group, and each d_{α_p} represents the physical sensor position of 2nd-group. Each sensor allocated at d_{α_p} produces the difference elements up to $d_{\alpha_p - (N/2 - 1)}$ and the sum elements up to $d_{\alpha_p + (N/2 - 1)}$ without holes. Therefore, the generated virtual elements are continuously lined and do not overlap each other as much as possible if we install actual sensors with no less than $(N - 1)d$ distance between every d_{α_p} position. For this reason, the condition

$$\begin{aligned} d_{\alpha_{p+1}} - d_{\alpha_p} &\geq (N - 1)d, \\ \text{where } d_{\alpha_{p+1}} &> d_{\alpha_p}, \quad 1 \leq p \leq N/2 - 1 \end{aligned} \quad (11)$$

is required, and the condition $\{d_{\alpha_{p+1}} - d_{\alpha_p} = (N - 1)d\}$ is desirable when we need to arrange without holes. Here, the sequences $\{d_0, \dots, d_{N-2}\}$ of the 1st-group and $\{d_{\alpha_{p+1}} - d_{\alpha_p} = d_{N-1}\}$ of the 2nd-group are well-connected. We chose the difference component $d_{\alpha_1 - (N/2 - 1)}$ of d_{α_1} to maintain the continuous allocation, so every position of d_{α_p} is determined with $(N - 1)d$ intervals. Figure 2 shows the 2-level sum and difference composite co-array configuration with even elements, which is formulated as

$$\begin{aligned} d_p &= pd, \quad (0 \leq p \leq N/2 - 1), \quad (1\text{st-level}), \quad (12) \\ d_{\alpha_p} &= \{(N - 1) + N/2 + (p - 1)(N - 1)\}d \\ &= \{N/2 + p(N - 1)\}d \\ &= \alpha_p d, \quad (1 \leq p \leq N/2), \quad (2\text{nd-level}). \end{aligned} \quad (13)$$

When the continuous virtual array elements in positive positions are more than or equal to $\alpha_{N/2} + (N/2 - 1) + 1 = (N + 1)N/2$, the virtual element at $d_{\alpha_1} + d_{\alpha_{N/2-1}}$ position is also connected as the farthest position element. In addition, the array elements at 0 and negative directions can also be created (discussed in Sect. 3.3), and more than or equal to $N_2 = 2\{(N + 1)N/2\} + 1 = (N + 1)N + 1$ virtual components appear continuously. We compare the DOF of the proposed method $\text{DOF}_{\text{Sum-Diff}} = (N + 1)N$ with the ideal maximum DOF of the difference co-array $\text{DOF}_{\text{Diff-Max}} = N(N - 1) + 1$ and find that it has the advantage of $(2N + 1)$ elements expansion; in other words, $1 + (2N - 1)/(N^2 - N + 1)$ times expansion. It expands by 1.54 times in the case of $N = 4$ and 1.35 times in the case of $N = 6$. The proposed method has an advantage in the case of small values of N , which are often used in real array applications.

Also, when compared with the DOF of the nested array $N_1 = (N^2/2 + N - 1)$, the proposed method has the advantage of $(N^2/2 + 1)$ elements expansion, which means $2 - (N - 2)/(N^2/2 + N - 1)$ times expansion. It expands by 1.82 times in the case of $N = 4$ and 1.87 times in the case of $N = 6$. Figure 3 compares the number of virtual elements as a function of the number of physical elements in each

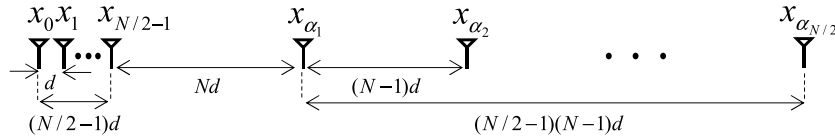


Fig. 2 Construction of N -element sum and difference co-array.

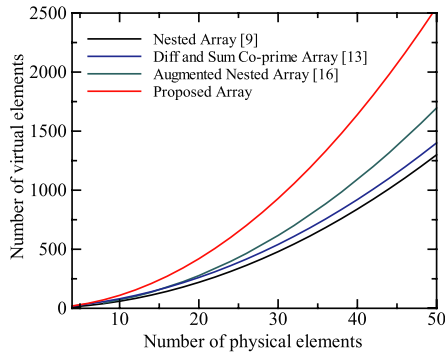


Fig. 3 Comparison of the numbers of physical and virtual elements.

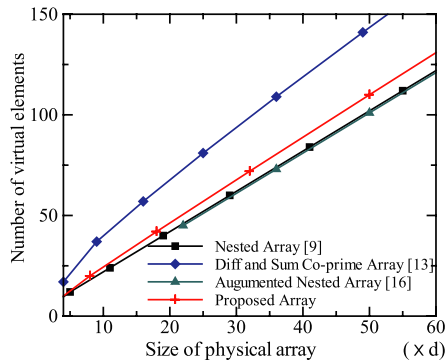


Fig. 4 Comparison of the physical array size and the numbers of virtual elements.

method. We see from Fig. 3 that the proposed array configuration achieves the largest number of virtual elements. We can confirm that the proposed method is more effective than the conventional methods in terms of the DOF for the number of physical elements.

Figure 4 also compares the number of virtual elements as a function of the physical array size (aperture). We see from Fig. 4 that the difference and sum co-prime array [13] achieves the largest number of virtual elements per the array size, and the proposed method is the 2nd largest. However, as discussed before with Fig. 3, the proposed approach looks the most effective from the viewpoint of the number of virtual element increments per physical elements (equivalent to the distance between the marker symbols in Fig. 4, as each marker shows the case of adding two more physical elements). Choosing either the difference and sum co-prime array [13] or the proposed array will depend on which is regarded as more important factor, the number of physical elements or the physical array size.

3.3 Practical Example of 6-Element Configuration

Let us consider array sensors with the positions of d_p, d_q where $\{p, q\} = \{0, 1, 2, 8, 13, 18\}$ as an example. The components expressed by the difference set of d_p and d_q become the following 27 positions:

$$\begin{aligned} \{q - p\} = \{-18, -17, -16, -13, -12, -11, -10, \\ -8, -7, -6, -5, -2, -1, 0, 1, 2, 5, 6, 7, \\ 8, 10, 11, 12, 13, 16, 17, 18\}. \end{aligned} \quad (14)$$

The elements described by the addition become the following 18 positions:

$$\begin{aligned} \{q + p\} = \{0, 1, 2, 3, 4, 8, 9, 10, 13, 14, 15, 18, \\ 19, 20, 21, 26, 31, 36\}. \end{aligned} \quad (15)$$

Note that this method enables us to express some additional positions that cannot be realized by the difference co-array. However, the above set does not include negative values.

Recall that the conjugate of the array steering vector becomes $a_p^*(\theta_i) = a_{-p}(\theta_i)$ and this expression represents the negative positions. The same as with the discussion on $a_p^*(\theta_i)a_q^*(\theta_i)$, we have

$$\check{\mathbf{R}}_{xx} = E[\mathbf{x}^*(k)\mathbf{x}^H(k)]. \quad (16)$$

$$\check{\mathbf{z}} = \text{vec}(\check{\mathbf{R}}_{xx}) \quad (17)$$

Again, the necessary condition for the desired plane signal $s_s(k)$ is real-valued. Then, the sum co-array can express the following 35 positions including the negative directions:

$$\begin{aligned} \{q + p\} \cup \{-(q + p)\} \\ = \{-36, -31, -26, -21, -20, -19, -18, -15, -14, \\ -13, -10, -9, -8, -4, -3, -2, -1, 0, 1, 2, 3, 4, 8, \\ 9, 10, 13, 14, 15, 18, 19, 20, 21, 26, 31, 36\}. \end{aligned} \quad (18)$$

Moreover, the above set contains more positions than that of the difference co-array from the reference point under ℓ_1 -norm (in the above case, less than -18 and more than 18). The extended virtual elements expressed by both of the sets (14) and (18) give us a total of 49 possible locations including 43 continuous components from -21 to 21 , as follows:

$$\begin{aligned} \{q - p\} \cup \{q + p\} \cup \{-(q + p)\} \\ = \{-36, -31, -26, -21, -20, \dots, 20, 21, 26, 31, 36\}. \end{aligned} \quad (19)$$

As a result, the extended sum and difference ‘‘composite’’ co-array elements exist continuously from -21 to 21 ,



Fig. 5 Construction of 6-element sum and difference co-array.

and $\text{DOF}_{\text{Sum-Diff}}$ is raised to 42 in this case. The result of $\text{DOF}_{\text{Sum-Diff}} = 42$ is about 4/3 times greater than $\text{DOF}_{\text{Diff-Max}} = N(N-1) + 1 = 31$ in the case of the 6-element array.

Figure 5 shows an example configuration of the proposed 6-element sum and difference composite co-array, where the red elements express the sensors that can be described only by the sum co-array. The concept of the proposed array configuration is based on interpolating the holes in the difference co-array with the help of the sum co-array, and consequently it can create a long continuous array element configuration.

4. Discussion

4.1 Application to MVDR Beamforming

As an application, we simulate MVDR beamforming in the next section to determine how the proposed co-array works. The extended input vector $\bar{\mathbf{z}} = [\mathbf{z}^T, \bar{\mathbf{z}}^T, \bar{\mathbf{z}}^T]^T \in \mathbb{C}^{3N^2 \times 1}$ corresponds to the power of the extended array, and we consider the beamforming via the weight vector $\bar{\mathbf{w}} = [\mathbf{w}_{\text{Diff}}^T, \mathbf{w}_{\text{Sum-Pos}}^T, \mathbf{w}_{\text{Sum-Neg}}^T]^T \in \mathbb{C}^{3N^2 \times 1}$. Its signal model is described as

$$\begin{aligned} y &= \bar{\mathbf{w}}^H \bar{\mathbf{z}} \\ &= \left\{ \sum_{i=1}^D \mathbf{w}_{\text{Diff}}^H (\mathbf{a}^*(\theta_i) \otimes \mathbf{a}(\theta_i)) \sigma_i^2 \right\} + \sigma^2 \mathbf{w}_{\text{Diff}}^H \mathbf{1}_N \\ &+ \left\{ \sum_{i=1}^D \mathbf{w}_{\text{Sum-Pos}}^H (\mathbf{a}(\theta_i) \otimes \mathbf{a}(\theta_i)) \tilde{\sigma}_i^2 \right\} + \tilde{\sigma}^2 \mathbf{w}_{\text{Sum-Pos}}^H \mathbf{1}_N \\ &+ \left\{ \sum_{i=1}^D \mathbf{w}_{\text{Sum-Neg}}^H (\mathbf{a}^*(\theta_i) \otimes \mathbf{a}^*(\theta_i)) \check{\sigma}_i^2 \right\} + \check{\sigma}^2 \mathbf{w}_{\text{Sum-Neg}}^H \mathbf{1}_N, \end{aligned} \quad (20)$$

where the terms \mathbf{w}_{Diff} , $\mathbf{w}_{\text{Sum-Pos}}$, $\mathbf{w}_{\text{Sum-Neg}}$ mean the weight vector of the difference co-array, that of the sum co-arrays for positive direction, and that for negative direction, respectively. The parameters σ_i^2 , $\tilde{\sigma}_i^2$, $\check{\sigma}_i^2$ describe the energies of the extended signals which comes from i -th DOA on the difference co-array and the sum co-arrays for positive and negative directions, respectively. Then, the weight vector $\bar{\mathbf{w}}_{\text{MVDR}} \in \mathbb{C}^{N^2 \times 1}$ in the MVDR beamformer is expressed as the solution of an optimization problem under the condition of the constraint:

$$\bar{\mathbf{w}}_{\text{MVDR}} = \frac{\bar{\mathbf{R}}_{\text{DL}}^{-1} \bar{\mathbf{a}}_1(\theta_1)}{\bar{\mathbf{a}}_1(\theta_1)^H \bar{\mathbf{R}}_{\text{DL}}^{-1} \bar{\mathbf{a}}_1(\theta_1)}, \quad (21)$$

where

$$\bar{\mathbf{R}}_{\text{DL}} = \bar{\mathbf{R}}_{\mathbf{z}\mathbf{z}} + \delta \mathbf{I}_{N^2} \in \mathbb{C}^{N^2 \times N^2}, \quad (22)$$

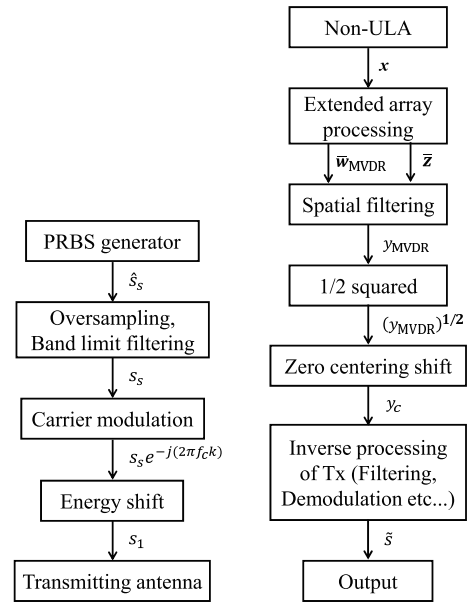


Fig. 6 Tx and Rx system models of simulations.

$$\bar{\mathbf{R}}_{\mathbf{z}\mathbf{z}} = \bar{\mathbf{z}}_1 \bar{\mathbf{z}}_1^H, \quad (23)$$

where $\bar{\mathbf{z}}_1 \in \mathbb{C}^{N^2 \times 1}$ denotes the shortened vector from $\bar{\mathbf{z}}$ by removing repeated rows, as to shorten \mathbf{z} into \mathbf{z}_1 in (4). Besides, the vector $\bar{\mathbf{a}}_1(\theta_1) \in \mathbb{C}^{N^2 \times 1}$ is the ideal steering vector without repeated elements to the desired wave direction θ_1 . This will lead to more robust beamforming performance as seen in the next section, and also has the great advantage that we can keep the DOF without any spatial smoothing method.

4.2 System Configuration

Figure 6 shows a transmitter (Tx) system model of the proposed beamformer. We first generate the symbol sequence $\hat{s}_s(k)$ as a pseudo random signal of BPSK, and then the sequence $\hat{s}_s(k)$ is filtered into $s_s(k)$ by using a root-cosine rolloff filter after oversampling to avoid any problems caused by Inter Symbol Interference (ISI). After that, the carrier wave $e^{-j(2\pi f_c k)}$ is multiplied to $s_s(k)$ and then transmitted from the transmission antenna. Note that the center value of the amplitude is shifted to 1 to avoid negative amplitudes for squared extended array operation, i.e., $s_1(k) = s_s(k)e^{-j(2\pi f_c k)} + 1$. This amplitude allocated in a positive quadrant works effectively; indeed, we do not have to distinguish whether squared signals were originally positive or not.

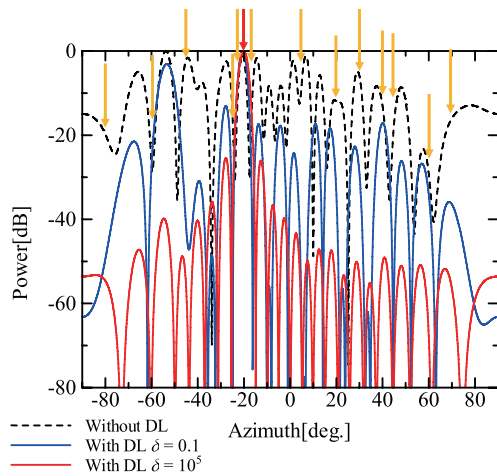
In the receiver (Rx) system shown in Fig. 6(b), we do not have to distinguish if the squared value was originally positive or not. The weights $\bar{\mathbf{w}}_{\text{MVDR}}$ and the extended signal $\bar{\mathbf{z}}$ are used to recover the output signal $\bar{s} \approx \hat{s}_s$ by spatial filtering. Note that the number of snapshots used in the autocorrelation process (2) and (3) should be within a symbol period, and is often common (but could be different) for

Table 1 Specifications of simulation no. 1.

Array configuration	Nested array
No. of array elements N	6
Sensor allocations $\{p, q\}$	$\{0, 1, 2, 3, 7, 11\}$
No. of input signals D	14
Array interval d_1	$\lambda/2$
Modulation	BPSK
DOA of desired wave	-20°
DOAs of interference waves	$-80^\circ, -60^\circ, -45^\circ, -25^\circ, -22^\circ, -18^\circ, 5^\circ, 20^\circ, 30^\circ, 40^\circ, 45^\circ, 60^\circ, 70^\circ$
SNR	10 dB
SIR	-3 dB
No. of snapshots	500

Table 2 Specifications of simulation no. 2.

No. of array elements N	6
Sensor allocations $\{p, q\}$	
Nested array	$\{0, 1, 2, 3, 7, 11\}$
Proposed array	$\{0, 1, 2, 8, 13, 18\}$
No. of input signals D	14
Array interval d_1	$\lambda/2$
Modulation	BPSK
DOA of desired wave	-20°
DOAs of interference waves	$-80^\circ, -60^\circ, -45^\circ, -25^\circ, -22^\circ, -18^\circ, 5^\circ, 20^\circ, 30^\circ, 40^\circ, 45^\circ, 60^\circ, 70^\circ$
SNR	-20 to 20 dB
SIR	20 dB (ex. 1), 10 dB (ex. 2)
No. of snapshots	500

**Fig. 7** Example beamforming results for 6-element nested array with and without DL method.

the generating processes of the weight vector $\bar{\mathbf{w}}_{\text{MVDR}}$ in (21) and the extended signal vector $\bar{\mathbf{z}}$ in (3). Then, we transform the spatial filtered output y_{MVDR} containing powered behaviors into the original amplitude expression by means of the square-root operation. The output y_c is acquired by the zero-centering shift operation, and now we use the temporal average of $(y_{\text{MVDR}})^{1/2}$ as an example of shift operator. After that, we apply the inverse processing of Tx, which includes the carrier wave rejection by multiplying the phase-term $e^{j(2\pi f_c k)}$, the root-cosine rolloff filtering, and the decimation. As a result, the processed output signal $\hat{s}(k)$ is obtained. In the next section, it is compared with the ideal source symbol sequence $\hat{s}_s(k)$ in terms of BER performance.

5. Simulation

In this section, we evaluate the performance of the proposed array configuration through computer simulation.

5.1 Effect of Diagonal Loading (DL)

First, we clarify the effect of the DL method (described in Sect. 4.1). The nested array often utilizes spatial smoothing to solve the rank deficiency problem of the array covariance

matrix. However, in the case of high SNRs or a small number of snapshots, the covariance matrix \mathbf{R}_{xx} becomes unstable and rank deficient. It may result in an undesired mainlobe direction or large sidelobes. Here, we confirm that the application of DL will solve the rank deficient problem and produce desired beamforming results. Specifications of the simulation are listed in Table 1. We used BPSK modulation to both desired and interference signals. Modulation of interference signals does not affect to beamforming result; we can also suppress complex digital modulations like QPSK or QAMs. Case of desired signal with complex modulation remains as one of future studies.

Figure 7 shows the beamforming results, where the red and yellow arrows respectively suggest the desired and interference directions. We see from Fig. 7 that the method without DL could not focus the mainlobe only to the desired direction. The DL method with a small value of δ ($= 0.1$) could focus the mainlobe but still has large sidelobes. The DL method with a large value of δ ($= 10^5$ or larger) sufficiently suppresses the sidelobe level and can make null beams to the interference directions, thus demonstrating that the DL works effectively.

5.2 Evaluation of the Proposed Array Configuration

Next, we compare the performance of the proposed array configuration and the nested array. Specifications of the simulation are listed in Table 2, where the same six elements are used but allocated to different positions.

Figure 8 shows the beam patterns formed by the proposed and conventional nested array configurations under the specifications in Table 2. Note that the DL method is applied to both the proposed and conventional nested arrays and we apply $\delta = 10^5$ to both configurations. We see from Fig. 8 that the proposed method can make better beam characteristics. As a result of creating a higher number of virtual array elements and enhancing the DOF, the proposed method can make 42 nulls while the conventional nested array makes only 22. Moreover, the narrow mainbeam width enables us to distinguish the close angles of -20° (desired) and $-18^\circ, -22^\circ$ (interference), so we conclude that this character works effectively in this simulation. Figure 8 also

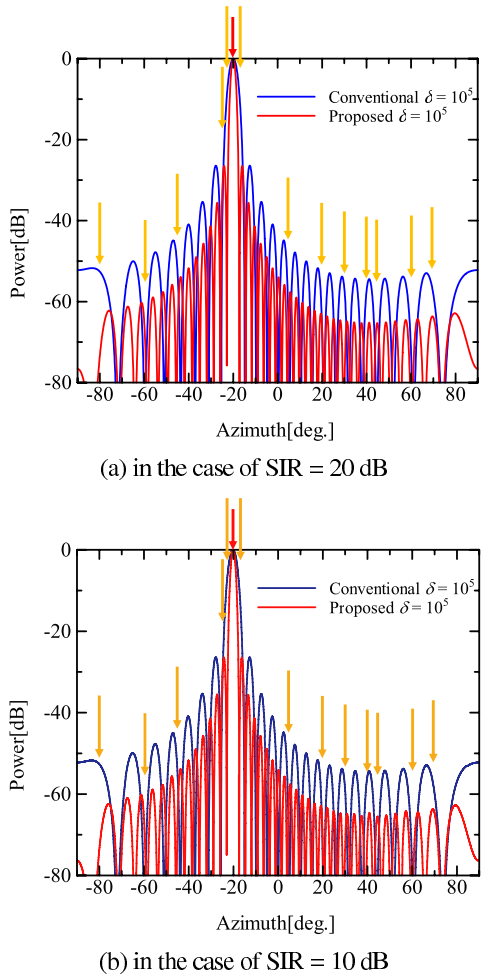


Fig. 8 Comparison of beam patterns for SNR = 20 dB.

shows that the sidelobe levels are well suppressed by the proposed array configuration. The effect of DL is robust but quite powerful, as Figs. 8(a) and (b) have similar characteristics.

Next, we evaluate BER to determine the performance of the whole array system (Figs. 6(a) and (b)). Figure 9(a) compares the BER performance in the case of 13 interference waves (Table 2). We can see from Fig. 9(a) that the proposed approach achieves a much better BER than the others in the case of an appropriate value $\delta = 10^5$ when $\text{SNR} > -15$ dB. Also, we can see from Fig. 9(b) that the proposed method works efficiently even under bad conditions (e.g., SIR = 0 dB).

We also evaluate the BER characteristics in a situation where the number of interference waves is changed: (a) six interferences from the DOAs of $\{-60^\circ, -45^\circ, -22^\circ, -18^\circ, 20^\circ, 30^\circ\}$ and (b) 29 interferences from the DOAs of $\{-40^\circ, -35^\circ, -30^\circ, -27^\circ, -23^\circ, -15^\circ, -12^\circ, -10^\circ, -5^\circ, 0^\circ, 10^\circ, 15^\circ, 55^\circ, 60^\circ, 80^\circ, 85^\circ\}$, plus 13 DOAs used in Fig. 9. The results are respectively shown in Figs. 10(a) and (b). We can see from Fig. 10 that the proposed method again achieves a better BER performance, and its characteristics are similar to the case of the 13 interfer-

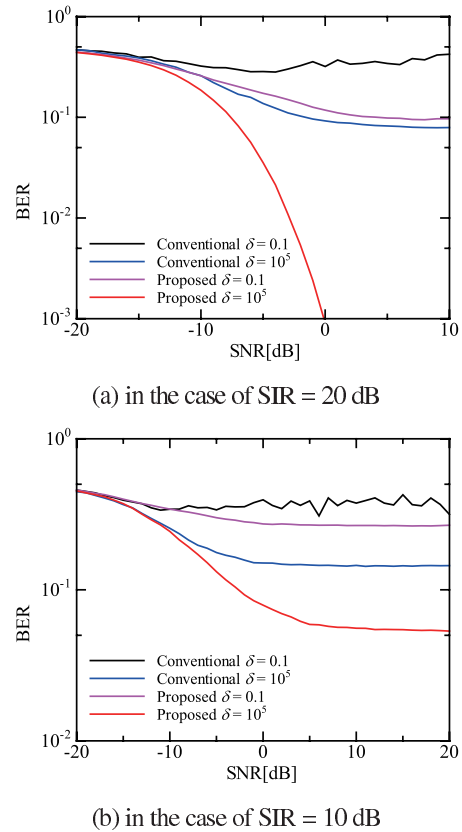


Fig. 9 Comparison of BER characteristics for 13 interference waves.

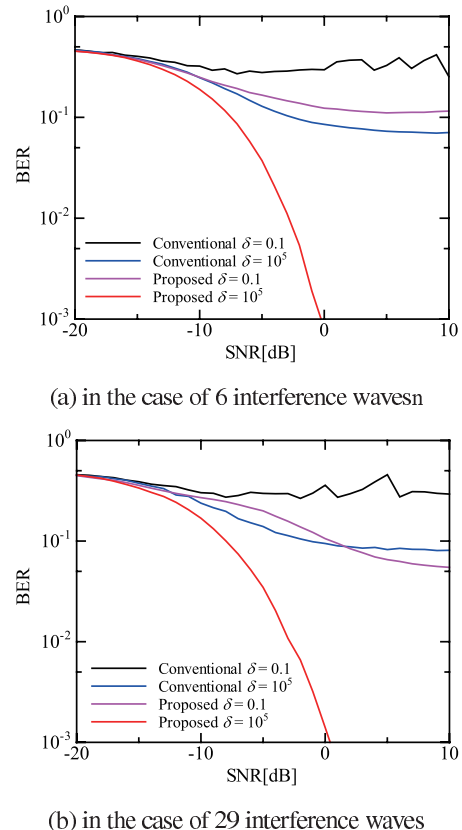


Fig. 10 Comparison of BER characteristics for SIR = 20 dB.

ence waves in Fig. 9. These results demonstrate that the proposed method is solid and robust, and that it can suppress interference waves coming from the close-angles with the desired signal.

6. Concluding Remarks

In this paper, we presented a novel array configuration called a “sum and difference composite co-array” based on the combination of the sum and difference co-arrays. The proposed array could further enhance the DOF and make better beam patterns with narrow mainlobe widths and a higher number of nulls beams. The results of computer simulation showed that the proposed array configuration had a better BER performance than the conventional configuration. Evaluating the DOA estimation performance of the proposed array configuration remains our future work.

Acknowledgments

This work was supported in part by the Telecommunication Advancement Foundation, the Support Center for Advanced Telecommunications Technology Research Foundation, and a JSPS Grant-in-Aid for Scientific Research no. 16K06381. The authors are sincerely grateful for their support.

References

- [1] B. Allen and M. Ghavami, *Adaptive Array Systems: Fundamentals and Applications*, Wiley, 2005.
- [2] C.A. Balanis and P.I. Ioannides, *Introduction to Smart Antennas*, Morgan & Claypool, 2007.
- [3] S. Chandran ed., *Adaptive Antenna Arrays: Trends and Applications*, Springer, 2004.
- [4] R.O. Schmidt, “Multiple emitter location and signal parameter estimation,” *IEEE Trans. Antennas Propag.*, vol.34, no.3, pp.276–280, March 1986.
- [5] R.T. Hoctor and S.A. Kassam, “The unifying role of the coarray in aperture synthesis for coherent and incoherent imaging,” *Proc. IEEE*, vol.78, no.4, pp.735–752, April 1990.
- [6] M.M. Hyder and K. Mahata, “Direction-of-arrival estimation using a Mixed $\ell_{2,0}$ norm approximation,” *IEEE Trans. Signal Process.*, vol.58, no.9, pp.4646–4655, Sept. 2010.
- [7] M.C. Dogan and J.M. Mendel, “Applications of cumulants to array processing Part I: Aperture extension and array calibration,” *IEEE Trans. Signal Process.*, vol.43, no.5, pp.1200–1216, May 1995.
- [8] W.K. Ma, T.H. Hsieh, and C.Y. Chi, “DOA estimation of quasi-stationary signals via Khatri-Rao subspace,” *IEEE Proc. Int. Conf. Acoustic. Speech Signal Process.*, pp.2165–2168, April 2009.
- [9] P. Pal and P.P. Vaidyanathan, “Nested arrays: A novel approach to array processing with enhanced degrees of freedom,” *IEEE Trans. Signal Process.*, vol.58, no.8, pp.4167–4181, Aug. 2010.
- [10] P. Pal and P.P. Vaidyanathan, “Nested arrays in two dimensions, Part I: geometrical considerations,” *IEEE Trans. Signal Process.*, vol.60, no.9, pp.4694–4705, Sept. 2012.
- [11] P.P. Vaidyanathan and P. Pal, “Sparse sensing with co-prime samplers and arrays,” *IEEE Trans. Signal Process.*, vol.59, no.2, pp.573–586, Feb. 2011.
- [12] Z. Tan, Y.C. Eldar, and A. Nehorai, “Direction of arrival estimation using co-prime arrays: A super resolution viewpoint,” *IEEE Trans. Signal Process.*, vol.62, no.21, pp.5565–5576, Nov. 2014.
- [13] X. Wang, Z. Chen, S. Ren, and S. Cao, “DOA estimation based on the difference and sum coarray for coprime arrays,” *Digit. Signal Process.*, vol.69, pp.22–31, Oct. 2017.
- [14] X. Wang, X. Wang, and X. Lin, “Co-prime array processing with sum and difference co-array,” *Proc. 49th Asilomar Conf. Signals, Systems and Computers*, pp.380–384, Nov. 2015.
- [15] Y. Huang, G. Liao, J. Li, J. Li, and H. Wang, “Sum and difference coarray based MIMO radar array optimization with its application for DOA estimation,” *Multidim. Syst. Sign. Process.*, vol.28, no.4, pp.1183–1202, Oct. 2017.
- [16] J. Liu, Y. Zhang, Y. Lu, S. Ren, and S. Cao, “Augmented nested arrays with enhanced DOF and reduced mutual coupling,” *IEEE Trans. Signal Process.*, vol.65, no.21, pp.5549–5563, Nov. 2017.
- [17] S. Iwazaki and K. Ichige, “Sum and difference composite co-array: An extended array configuration toward higher degree of freedom,” *Proc. International Conference on Advances in Electrical, Electronic and Systems Engineering (ICAEESE)*, pp.351–356, Nov. 2016.
- [18] S. Iwazaki and K. Ichige, “Extended beamforming by sum and difference composite co-array for radio surveillance,” *Proc. IEEE International Workshop on Information Forensics and Security (WIFS)*, no.61, Dec. 2017.
- [19] S.U. Pillai and B.H. Kwon, “Forward/backward spatial smoothing techniques for coherent signal identification,” *IEEE Trans. Acoust., Speech Signal Process.*, vol.37, no.1, pp.8–15, Jan. 1989.



Sho Iwazaki received the B.E. and M.E. degrees in Electrical and Computer Engineering from Yokohama National University in 2009 and 2011, respectively. He joined Sony Corporation in 2011 and currently on loan to Sony Interactive Entertainment Inc. from 2015. He also holds a position of a doctoral student in Yokohama National University from 2015. His research interests include array signal processing and its applications. He received Best Student Paper Award in Int. Conf. on Electrical, Electronic and Systems Engineering (ICAEESE) in 2016.



Koichi Ichige received B.E., M.E. and Dr. Eng. degrees in Electronics and Computer Engineering from the University of Tsukuba in 1994, 1996 and 1999, respectively. He joined the Department of Electrical and Computer Engineering, Yokohama National University as a research associate in 1999, where he is currently a professor. He has been on leave to Swiss Federal Institute of Technology Lausanne (EPFL), Switzerland as a visiting researcher in 2001–2002. His research interests include digital signal processing, approximation theory and their applications to image processing and mobile communication. He served as an associate editor of *IEEE Transactions on Industrial Electronics* in 2004–2008, *Journal of Circuits, Systems and Computers (JCSC)* in 2012–2014, and *IEICE Transactions on Fundamentals of Electronics, Communications and Computer Sciences* in 2015–2018. He received “Meritorious Award on Radio” from the Association of Radio Industries and Businesses (ARIB) in 2006, and Best Letter Award from IEICE Communication Society in 2007. He is a member of IEEE.